JOINT TIME SYNCHRONIZATION AND LOCALIZATION FOR TARGET SENSORS USING A SINGLE MOBILE ANCHOR WITH POSITION UNCERTAINTIES

Fangling Yao, Yiyin Wang, and Xinping Guan

The Dept. of Automation Shanghai Jiao Tong University
Collaborative Innovation Center for Advanced Ship and Deep-Sea Exploration(CISSE)
Key Laboratory of System Control and Information Processing, Ministry of Education of China
Shanghai 200240, China

ABSTRACT

Clock synchronization is required by most time-based localization methods in wireless sensor networks (WSNs). However, synchronization is often coupled with localization. Furthermore, the accuracy of anchor positions depends on several factors, and uncertainties may exist in the observed anchor positions. Thus, we propose a joint time and location estimation of target sensors using a single mobile anchor to reduce the deployment cost for WSNs. Taking anchor position uncertainties into account, we develop an expectation maximization (EM)-type method to solve the joint estimation problem. The simulation results verify the performance of the proposed EM method is superior than conventional methods, such as generalized total least squares (GTLS) and least squares (LS) estimators.

Index Terms— wireless sensor networks, expectation maximization, localization, synchronization, anchor position uncertainties

1. INTRODUCTION

Wireless sensor networks (WSNs) attract numerous attention because of their wide applications [1] [2]. The information gathered by sensors will be much more meaningful if it is tagged with sensor positions and timestamps to indicate where and when it is collected. Thus it is significant to solve localization and synchronization problems for WSNs. Time-based approaches are often adopted in localization for WSNs. However, time synchronization is always coupled with time-based localization. Furthermore, anchor positions are often determined by global positioning system (GPS), inertial navigation system (INS) [3] or baseline localization systems [4]. The uncertainties of anchor positions are inevitable and degrade the localization and synchronization performance of target sensors.

In order to deal with the coupled problems, some research works propose to accomplish localization and time synchronization simultaneously. For instance, in [5] and [6], the joint estimation is accomplished by semi-definite programming (SDP). Moreover, a distributed belief propagation algorithm is developed in [7]. A novel two-step algorithm is described in [8]. However, none of these algorithms considers anchor position uncertainties. To cope with anchor position uncertainties, [9] and [10] propose the target position estimation for WSNs through SDP and expectation maximization (EM), respectively. However neither of them considers synchronization issues. In addition, some research works propose to accomplish the joint estimation with anchor position uncertainties. In [11] an semi-definite relaxation (SDR) method is proposed. However, the estimation of clock skew is not taken into account. Referring to our previous work introduced in [12], we develop our scheme as follows.

In this paper, we use a single mobile node as an anchor node to assist the localization and synchronization of target sensors. Instead of fixing anchor nodes in WSNs, the mobile anchor decreases the anchor deployment cost and adds flexibility. On the other hand, anchor position uncertainties introduce errors in localization and synchronization. We adopt the EM algorithm to accomplish the joint estimation with anchor position uncertainties. We also tailor the conventional generalized total least squares (GTLS) and least square (LS) estimators to compare with the proposed EM method.

The rest of this paper is organized as follows. In Section 2, the system model of joint synchronization and localization in the presence of anchor position uncertainties is presented. In Section 3, we propose the EM algorithm and adjust the GTLS and LS algorithms for fair comparison. The root mean square error (RMSE) of the proposed EM estimator is compared with the ones of the LS and GTLS algorithms in Section 4.

2. SYSTEM MODEL

We consider a scenario where a single mobile anchor is employed to help localization and synchronization of target sensors in WSNs. As the proposed method is the same for all the sensor nodes, we exemplify the case of localization and synchronization of a single target sensor. The position and timestamp of the mobile anchor is recorded whenever it broadcasts a packet. If we assume that the mobile anchor has a standard clock with a reference time t, and the target sensor has an asynchronous clock with its local time $C(t)$, their relationship can be given as follows.

$$C(t) = \alpha t + \beta, \tag{1}$$

where α is the clock skew, and β is the clock offset of the target sensor with respect to (w.r.t.) the mobile anchor. We define that the i-th packet is broadcast by the mobile anchor at t_i according to the standard clock. The current mobile anchor position is recorded as $\mathbf{a}_i$. The relationship among $\mathbf{a}_i$, $\mathbf{a}_{io}$ and $\Delta\mathbf{a}_i$ is described as $\mathbf{a}_{io} = \mathbf{a}_i + \Delta\mathbf{a}_i$, where $[\Delta\mathbf{a}_i]_j \sim N(0, \sigma_a^2)$. As presented in Fig.1, the

Part of this work was supported by the National Nature Science Foundation of China under the grants 61773264, 61633017, and 61471237.

mobile anchor moves along a user-defined trajectory, which is along the edges of a rectangular.

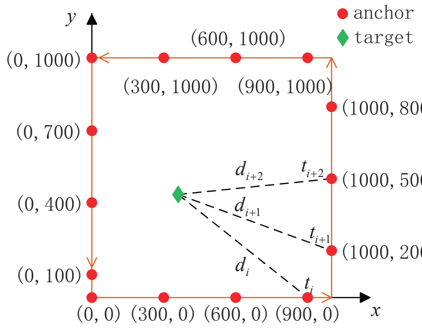

Fig. 1: An example of localizing a target sensor by a single mobile sensor.

According to the time of flight between the mobile anchor and the target sensor, the distance between them could be calculated. Define the position of the target sensor as $\mathbf{x}$. The distance between the target sensor and the mobile anchor while the i-th packet is broadcast can be defined as d_i, where $d_i = \|\mathbf{a}_{io} - \mathbf{x}\|$. We consider the system of two dimensions, which could be extended to the three dimensional case easily. The time stamp r_i is recorded when the i-th packet is received by the target sensor and is modeled as follows.

$$r_i = \alpha(t_i + \frac{d_i + w_i}{c}) + \beta, \tag{2}$$

where c is the signal propagation speed related with environment conditions. The measurement noise is denoted as w_i, and $w_i \sim N(0, \sigma_w^2)$.

Let us define $\theta_1 = \dfrac{1}{\alpha}$ and $\theta_2 = \dfrac{\beta}{\alpha}$, and assume that there are N packets received by the target sensor. According to the linearization step in Appendix A.1, (2) can be rearranged into a linear equation as

$$\mathbf{b} = \mathbf{G}\mathbf{y} - \mathbf{A}\mathbf{h}_o + \mathbf{e}, \tag{3}$$

where $[\mathbf{b}]_i = c^2 t_i^2 + \|\mathbf{a}_i\|^2$, $\mathbf{G} = \begin{bmatrix} \mathbf{H}_o & \mathbf{S} \end{bmatrix}$, with $i = 1 \cdots N$,
$[\mathbf{H}_o]_{i,:} = -2\mathbf{a}_{io}^T$,
$[\mathbf{S}]_{i,:} = \begin{bmatrix} 2c^2 r_i t_i, & -2c^2 t_i, & 2c^2 r_i, & -c^2 r_i^2, & 1 \end{bmatrix}$,
$\mathbf{y} = \begin{bmatrix} \mathbf{x}^T & \mathbf{z}^T \end{bmatrix}^T$, with
$\mathbf{z} = \begin{bmatrix} \theta_1, & \theta_2, & \theta_1\theta_2, & \theta_1^2, & \|\mathbf{x}\|^2 - c^2\theta_2^2 \end{bmatrix}^T$,

$$\mathbf{A} = \begin{bmatrix} \mathbf{a}_1^T & \mathbf{0}_2^T & \cdots & \mathbf{0}_2^T \\ \mathbf{0}_2^T & \mathbf{a}_2^T & \cdots & \mathbf{0}_2^T \\ \vdots & \vdots & \ddots & \vdots \\ \mathbf{0}_2^T & \mathbf{0}_2^T & \cdots & \mathbf{a}_N^T \end{bmatrix}, \quad [\mathbf{h}_o] = vec(\mathbf{H}_o),$$

$[\mathbf{e}]_i = 2d_i w_i + w_i^2 + \|\Delta\mathbf{a}_i\|^2$.
Considering the relationship between elements of $\mathbf{H}_o$ and $\mathbf{h}_o$, the model (3) can also be rewritten as

$$\mathbf{b} = (\mathbf{I}_N \otimes \mathbf{x}^T - \mathbf{A})\mathbf{h}_o + \mathbf{S}\mathbf{z} + \mathbf{e}. \tag{4}$$

The EM-based method will be developed based on (4) in the following sections.

3. THE PROPOSED EM-BASED METHOD

This section proposes the EM algorithm to estimate the clock parameters and position of the target sensor. We also tailor the LS and GTLS estimators to compare with the EM-based method.

3.1. The iterative steps of the EM method

The EM algorithm tries to find the maximum likelihood estimation through iterative steps. This iterative algorithm aims to complete the estimation with data dropouts. The system model presented in (4) indicates that $\mathbf{y} = \begin{bmatrix} \mathbf{x}^T & \mathbf{z}^T \end{bmatrix}^T$ could be estimated if $\mathbf{b}$ and $\mathbf{h}_o$ are observed correctly. However, $\mathbf{h}_o$ is unknown due to anchor position uncertainties. Thus, we regard $\mathbf{h}_o$ as the hidden variable vector. We carry out the E step and M step of the EM algorithm respectively, after the initial value of $\mathbf{y}$ is determined by the LS estimator.

The E step

In this step, we compute the expectation to obtain the hidden variable vector estimation and the objective function of the EM algorithm. The estimation of $\mathbf{h}_o$ is determined by the expected value of $\mathbf{h}_o$ w.r.t. $\mathbf{b}$ and the previous estimate of $\mathbf{y}$ as $\widehat{\mathbf{y}}(k-1)$. This estimator is also called minimum mean square error (MMSE) estimator. The error covariance of the MMSE estimator is calculated as (6).

$$\widehat{\mathbf{h}}_o(k) = \int_{\mathbf{h}_o} \mathbf{h}_o p(\mathbf{h}_o|\mathbf{b}, \widehat{\mathbf{y}}(k-1)) d\mathbf{h}_o. \tag{5}$$

$$\begin{aligned} &\mathbf{C}_{\widehat{\mathbf{h}}_o}(k) \\ &= \int_{\mathbf{h}_o} (\mathbf{h}_o - \widehat{\mathbf{h}}_o(k))(\mathbf{h}_o - \widehat{\mathbf{h}}_o(k))^T p(\mathbf{h}_o|\mathbf{b}, \widehat{\mathbf{y}}(k-1)) d\mathbf{h}_o. \end{aligned} \tag{6}$$

The objective function of the EM algorithm is the expected value of $log\ p(\mathbf{b}, \mathbf{h}_o|\mathbf{y})$ w.r.t. the conditional distribution of $\mathbf{h}_o$ given $\mathbf{b}$ under $\widehat{\mathbf{y}}(k-1)$. If we denote the expected value of the log likelihood as $Q(\mathbf{y}|\widehat{\mathbf{y}}(k-1))$, it could be written as

$$Q(\mathbf{y}|\widehat{\mathbf{y}}(k-1)) = \int_{\mathbf{h}_o} (log\ p(\mathbf{b}, \mathbf{h}_o|\mathbf{y}))\ p(\mathbf{h}_o|\mathbf{b}, \widehat{\mathbf{y}}(k-1)) d\mathbf{h}_o. \tag{7}$$

Since $p(\mathbf{b}, \mathbf{h}_o|\mathbf{y}) = p(\mathbf{b}|\mathbf{h}_o, \mathbf{y}) p(\mathbf{h}_o|\mathbf{y})$ and $\mathbf{h}_o$ is independent from $\mathbf{y}$, we can simplify the calculation of $Q(\mathbf{y}|\widehat{\mathbf{y}}(k-1))$ through dropping the constant terms. Thus, the following equation can be easily obtained.

$$Q(\mathbf{y}|\widehat{\mathbf{y}}(k-1)) \propto \int_{\mathbf{h}_o} (log\ p(\mathbf{b}|\mathbf{h}_o, \mathbf{y}))\ p(\mathbf{h}_o|\mathbf{b}, \widehat{\mathbf{y}}(k-1)) d\mathbf{h}_o. \tag{8}$$

Using the Taylor expansion, (8) has a linear approximation at $\widehat{\mathbf{h}}_o(k)$, which is the current estimate of $\mathbf{h}_o$. As the higher-order terms are equal to zero, only the first two derivatives remain. Denote $\mathbf{C}_\mathbf{e}$ as the covariance matrix of $\mathbf{e}$, and $\mathbf{c}_l$ as the l-th column vector of the square root of $\mathbf{C}_\mathbf{e}$. Therefore, $[\mathbf{c}_l]_i = \begin{cases} \dfrac{1}{\sqrt{4d_i^2\sigma_w^2 + 2\sigma_w^4 + 2\sigma_a^4}}, & i = l \\ 0, & i \neq l \end{cases}$. Using (5) and (6), we could simplify $Q(\mathbf{y}|\widehat{\mathbf{y}}(k-1))$ as a quadratic function w.r.t. $\mathbf{y}$

$$\begin{aligned} &Q(\mathbf{y}|\widehat{\mathbf{y}}(k-1)) \\ &\propto (\mathbf{b} - (\mathbf{I}_N \otimes \mathbf{x}^T - \mathbf{A})\widehat{\mathbf{h}}_o(k) - \mathbf{S}\mathbf{z} - \mathbf{E}\{\mathbf{e}\})^T \mathbf{C}_e^{-1} \\ &(\mathbf{b} - (\mathbf{I}_N \otimes \mathbf{x}^T - \mathbf{A})\widehat{\mathbf{h}}_o(k) - \mathbf{S}\mathbf{z} - \mathbf{E}\{\mathbf{e}\}) \\ &+ \sum_{l=1}^{N} \mathbf{c}_l^T (\mathbf{I}_N \otimes \mathbf{x}^T - \mathbf{A}) \mathbf{C}_{\widehat{\mathbf{h}}_o}(k) (\mathbf{I}_N \otimes \mathbf{x}^T - \mathbf{A})^T \mathbf{c}_l. \end{aligned} \tag{9}$$

The M step
In this step, $\widehat{\mathbf{y}}(k)$ is achieved by maximizing (9). The estimate $\widehat{\mathbf{y}}(k)$ could be obtained if the derivative of (9) w.r.t. $\mathbf{y}$ equals to zero. Let us define $\widehat{\mathbf{G}}(k) = \left[\begin{array}{cc} \widehat{\mathbf{H}}_o(k) & \mathbf{S} \end{array} \right]$. As a result, we obtain the estimate of $\mathbf{y}$ in the current iteration as follows.

$$\begin{aligned}
&\widehat{\mathbf{y}}(k) \\
&= ((\widehat{\mathbf{G}}(k))^T \mathbf{C}_e^{-1} \widehat{\mathbf{G}}(k) + \sum_{k=1}^{N} \mathbf{P}^T (\mathbf{c}_l^T \otimes \mathbf{I}_2) \mathbf{C}_{\widehat{\mathbf{h}}_o(k)} (\mathbf{c}_l \otimes \mathbf{I}_2) \mathbf{P})^{-1} \\
&((\widehat{\mathbf{G}}(k))^T \mathbf{C}_e^{-1} (\mathbf{b} + \mathbf{A}\widehat{\mathbf{h}}_o(k) - \mathbf{E}\{\mathbf{e}\}) \\
&+ \sum_{k=1}^{N} \mathbf{P}^T (\mathbf{c}_l^T \otimes \mathbf{I}_2) \mathbf{C}_{\widehat{\mathbf{h}}_o}(k) \mathbf{A}^T \mathbf{c}_l), \qquad (10)
\end{aligned}$$

where $\mathbf{P} = \left[\begin{array}{cc} \mathbf{I}_2 & \mathbf{0}_{2\times 5} \end{array} \right]$, and $\mathbf{x} = \mathbf{P}\mathbf{y}$.

In summary, the estimation process consists of two steps. Firstly, $\widehat{\mathbf{h}}_o(k)$ and $\mathbf{C}_{\widehat{\mathbf{h}}_o}(k)$ is derived according to (22) and (23) in Appendix A.3 and we arrive at (9). Secondly, we could obtain $\widehat{\mathbf{y}}(k)$ through (10). The two steps are repeated alternately. The EM algorithm terminates when $\|\widehat{\mathbf{x}}(k) - \widehat{\mathbf{x}}(k-1)\| \leq 0.001$. The initial value $\widehat{\mathbf{y}}(0)$ comes from an LS estimator.

3.2. The tailored LS, WLS and GTLS estimators

In this section, we tailor the LS and GTLS estimators for joint time synchronization and localization with anchor position uncertainties. The performance of the two algorithms could be compared with the EM-based method.

The LS and WLS algorithm
Define $[\boldsymbol{\rho}]_i = c^2 t_i^2 - \|\mathbf{a}_i\|^2$, $[\boldsymbol{\epsilon}]_i = 2d_i w_i + w_i^2 + \|\Delta\mathbf{a}_i\|^2 + 2\mathbf{a}_i^T \Delta\mathbf{a}_i$, $\bar{\mathbf{y}} = \mathbf{y} + \Delta\bar{\mathbf{y}}, \Delta\bar{\mathbf{y}} = \left[\begin{array}{cc} \mathbf{0}_6^T & \sigma_w^2 + 2\sigma_a^2 \end{array} \right]^T$ and rewrite (3). We obtain the system model for the LS estimator and the LS estimate of $\bar{\mathbf{y}}$ as follows.

$$\boldsymbol{\rho} = \mathbf{G}\bar{\mathbf{y}} + \boldsymbol{\epsilon} - \mathbf{E}\{\boldsymbol{\epsilon}\} = \mathbf{G}\bar{\mathbf{y}} + \boldsymbol{\epsilon} - (\sigma_w^2 + 2\sigma_a^2)\mathbf{1}_N, \qquad (11)$$

$$\widehat{\bar{\mathbf{y}}}_{LS} = (\mathbf{G}^T\mathbf{G})^{-1}\mathbf{G}^T\boldsymbol{\rho}. \qquad (12)$$

Note that the accurate anchor position is unknown because of anchor position uncertainties, the value of $\mathbf{a}_{io}$ in submatrix $\mathbf{H}_o$ of $\mathbf{G}$ is replaced by $\mathbf{a}_i$ during the estimation process.

When the accurate positions of the mobile anchor are known, we denote $[\boldsymbol{\zeta}]_i = c^2 t_i^2 - \|\mathbf{a}_{io}\|^2$, $[\boldsymbol{\eta}]_i = 2d_i w_i + w_i^2$, $\tilde{\mathbf{y}} = \mathbf{y} + \Delta\tilde{\mathbf{y}}$, $\Delta\tilde{\mathbf{y}} = \left[\begin{array}{cc} \mathbf{0}_6^T & \sigma_w^2 \end{array} \right]^T$. We arrive at $\boldsymbol{\zeta} = \mathbf{G}\tilde{\mathbf{y}} + \boldsymbol{\eta}$ according to (18) in Appendix A.1. Denote the covariance matrix of $\boldsymbol{\eta}$ as $\boldsymbol{C}_{\boldsymbol{\eta}}$, which is a diagonal matrix and $[\boldsymbol{C}_{\boldsymbol{\eta}}]_{i,i} = 4d_i^2\sigma_w^2 + 2\sigma_w^4$. The value of d_i is decided by $d_i = \|\widehat{\bar{\mathbf{x}}}_{LS} - \mathbf{a}_{io}\|$. The LS and WLS estimate $\widehat{\tilde{\mathbf{y}}}_{LS-I}$ and $\widehat{\tilde{\mathbf{y}}}_{WLS}$ as follows, respectively.

$$\widehat{\tilde{\mathbf{y}}}_{LS-I} = (\mathbf{G}^T\mathbf{G})^{-1}\mathbf{G}^T\boldsymbol{\zeta} \qquad (13)$$

$$\widehat{\tilde{\mathbf{y}}}_{WLS} = (\mathbf{G}^T\boldsymbol{C}_{\boldsymbol{\eta}}{}^{-1}\mathbf{G})^{-1}\mathbf{G}^T\boldsymbol{C}_{\boldsymbol{\eta}}{}^{-1}\boldsymbol{\zeta}. \qquad (14)$$

The GTLS algorithm
Referring to [13], the GTLS solves the linear parameter estimation problem while the observation matrix has Gaussian noise with zero mean. The equation (3) is equivalent to (15) while $\vec{\mathbf{y}} = [\mathbf{y}]_{1:6}, \mathbf{W} = [\mathbf{G}]_{:,1:6}, [\boldsymbol{\varepsilon}]_i = 2d_i w_i + w_i^2 + \|\Delta\mathbf{a}_i\|^2 + 2\mathbf{a}_i^T\Delta\mathbf{a}_i + \|\mathbf{x}\|^2 - c^2\theta_2^2$.

$$\boldsymbol{\rho} = \mathbf{W}\vec{\mathbf{y}} + \boldsymbol{\varepsilon}. \qquad (15)$$

The expected value of $\boldsymbol{\varepsilon}$ is not equal to zero. Therefore, we substract $\mathbf{E}\{\boldsymbol{\varepsilon}\}$ from both sides of (15). Let us define $\boldsymbol{\varrho} = \boldsymbol{\rho} - \mathbf{E}\{\boldsymbol{\varepsilon}\}$. Considering the LS estimator is unbiased, the estimate of $\mathbf{E}\{\boldsymbol{\varepsilon}\}$ could be obtained by $[\widehat{\bar{\mathbf{y}}}_{LS}]_7$. Then, the following equation could be derived.

$$\boldsymbol{\varrho} = \mathbf{W}\vec{\mathbf{y}} + \boldsymbol{\varepsilon} - [\widehat{\bar{\mathbf{y}}}_{LS}]_7\mathbf{1}_N. \qquad (16)$$

Denote the errors in $\mathbf{H}_o$ and $\boldsymbol{\varrho}$ as $[\mathbf{F}]_{i,:} = \left[\begin{array}{cc} -2\Delta\mathbf{a}_{io}^T & [\boldsymbol{\varepsilon}]_i - [\widehat{\bar{\mathbf{y}}}_{LS}]_7 \end{array} \right]$ and $\mathbf{C}_{\mathbf{F}} = E\{\mathbf{F}^T\mathbf{F}\}$. $\mathbf{R}_C$ is the Cholesky decomposition of $\mathbf{C}_{\mathbf{F}}$. Therefore, the GTLS algorithm is proposed as

$$\begin{aligned}
&\arg\min_{\widehat{\mathbf{H}}_o, \widehat{\boldsymbol{\varrho}}} \left\| \left[\begin{array}{cc} \mathbf{H}_o - \widehat{\mathbf{H}}_o & \boldsymbol{\varrho} - \widehat{\boldsymbol{\varrho}} \end{array} \right] \mathbf{R}_C^{-1} \right\| \\
&s.t.\ Range(\widehat{\boldsymbol{\varrho}}) \subseteq Range(\widehat{\mathbf{W}}). \qquad (17)
\end{aligned}$$

The detailed solution procedure of this problem is described in [13].

4. PERFORMANCE EVALUATION

In this section, we evaluate the performance of the EM method through simulations in underwater WSNs. The positions of mobile anchor are decided by GPS when it is on the sea surface and INS underwater. Thus, the positions consist uncertainties. As the depth of the target sensor could be measured by pressure sensors, we consider the localization system of two dimensions. The accurate positions where the mobile anchor transmits signals are shown in Fig. 1. The signal propagation speed is $c = 1500$ m/s, which is the average speed of acoustic signal underwater. The coordinates of the target sensor are uniformly distributed inside the square in Fig. 1. The clock parameters α and β are uniformly distributed in the range $[-0.3, 0.3]$ and $[1 - 10^{-3}, 1 + 10^{-3}]$, respectively. We run 5000 rounds of Monte Carlo trails to obtain the simulation results.

Fig. 2 shows the position estimation performance versus different anchor position uncertainties, when $\sigma_w^2 = 10$ m^2. The EM estimator achieves the best performance compared with the LS and GTLS estimators. Because it explores the priori information about the anchor position and noise. The GTLS estimator performs better than the LS estimator as expected. The WLS estimator has a lower RMSE than the LS-I estimator though both of them are carried out based on accurate anchor positions. The EM algorithm performs better than the LS estimator even though the anchor position uncertainties are low. It is clear that the EM estimator has a better performance than LS-I while $1/\sigma_a^2$ is greater than 10 dB. Figs. 3 and 4 show the performance of clock skew and offset estimation under the same settings as in Fig. 2. The trend is similar to Fig. 2.

If we set $\sigma_a^2 = 10$ m^2, the RMSE of localization under different measurement noises could be illustrated in Fig. 5. The WLS estimator has a lower RMSE than LS-I and the gap between their performance stays constant. The error floors are determined by the anchor position uncertainties. The EM algorithm perform better than the LS-I estimator while $1/\sigma_w^2$ is more than 10 dB. The performance trend of clock skew and offset estimation under the same settings as in Fig. 5 is similar to the position estimation. Thus, we omit their figures.

A. APPENDIX

A.1. Linearization of (2)

Firstly, the equation in (2) could be rewritten as $(r_i\theta_1 - \theta_2 - t_i)c = d_i + w_i$. Squaring both sides of the equation, we could obtain

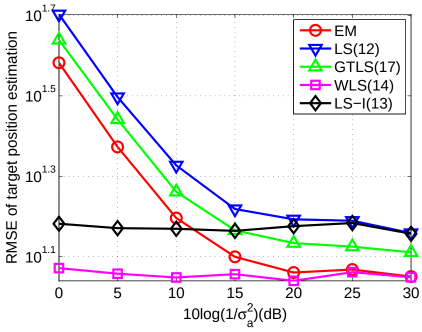

Fig. 2: RMSE of sensor position estimation

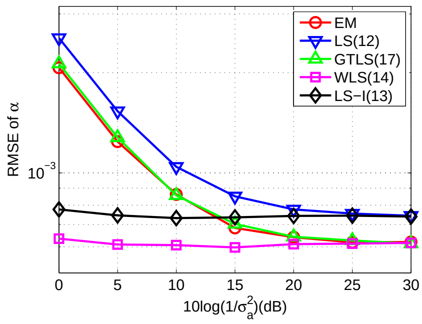

Fig. 3: RMSE of α estimation

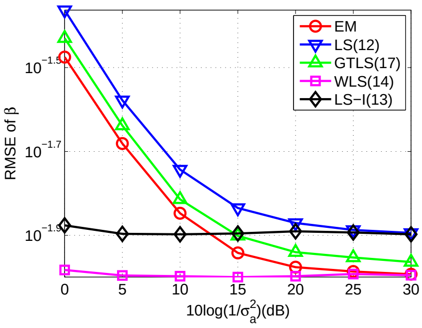

Fig. 4: RMSE of β estimation

$(r_i^2\theta_1^2+\theta_2^2+t_i^2-2r_i\theta_1\theta_2-2r_it_i\theta_1+2t_i\theta_2)c^2 = d_i^2+2d_iw_i+w_i^2$. According to $d_i = \|\mathbf{x}-\mathbf{a}_{io}\|$, the following equation could be computed.

$$\begin{aligned}&(r_i^2\theta_1^2+\theta_2^2+t_i^2-2r_i\theta_1\theta_2-2r_it_i\theta_1+2t_i\theta_2)c^2\\&=\|\mathbf{x}\|^2-2\mathbf{a}_{io}^T\mathbf{x}+\|\mathbf{a}_{io}\|^2+2d_iw_i+w_i^2.\end{aligned} \tag{18}$$

As $\mathbf{a}_{io} = \mathbf{a}_i + \Delta\mathbf{a}_i$, we could get $\|\mathbf{a}_{io}\|^2 = \|\mathbf{a}_i\|^2 + \|\Delta\mathbf{a}_i\|^2 + 2\mathbf{a}_i^T\Delta\mathbf{a}_i = -\|\mathbf{a}_i\|^2 + \|\Delta\mathbf{a}_i\|^2 + 2\mathbf{a}_i^T\mathbf{a}_{io}$. Thus, the equation as follow could be derived.

$$\begin{aligned}&c^2t_i^2+\|\mathbf{a}_i\|^2\\&=-2\mathbf{a}_{io}^T\mathbf{x}+2c^2r_it_i\theta_1-2c^2t_i\theta_2+2c^2r_i\theta_1\theta_2-c^2r_i^2\theta_1^2\\&+\|\mathbf{x}\|^2-c^2\theta_2^2+2\mathbf{a}_i^T\mathbf{a}_{io}+\|\Delta\mathbf{a}_i\|^2+2d_iw_i+w_i^2.\end{aligned} \tag{19}$$

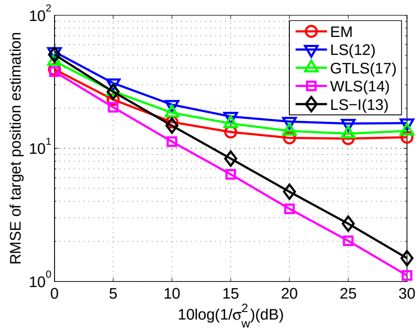

Fig. 5: RMSE of sensor position estimation

A.2. The covariance matrix $\mathbf{C_e}$ and $\mathbf{C_{h_o}}$

As $w_i \sim N(0,\sigma_w^2)$ and $[\Delta\mathbf{a}_i]_j \sim N(0,\sigma_a^2)$, the expectation and covariance matrix of $\mathbf{e}$ can be modeled as follows.

$$\mathbf{E}\{[\mathbf{e}]_i\} = \mathbf{E}\{2d_iw_i+w_i^2+\|\Delta\mathbf{a}_i\|^2\} = \sigma_w^2+2\sigma_a^2, \tag{20}$$

$$\begin{aligned}[\mathbf{C_e}]_{i,j} &= \mathbf{E}\{[\mathbf{e}]_i[\mathbf{e}]_j\} - \mathbf{E}\{[\mathbf{e}]_i\}\mathbf{E}\{[\mathbf{e}]_j\}\\ &= \begin{cases}4d_i^2\sigma_w^2+2\sigma_w^4+2\sigma_a^4 & i=j\\ 0 & i\neq j\end{cases},\end{aligned} \tag{21}$$

$\mathbf{C_e}$ is related to the distance d_i, and it should be updated upon the current estimate of $\mathbf{x}$ and $\mathbf{a}_{io}$ every iteration.

The covariance matrix $\mathbf{C_{h_o}}$ of $\mathbf{h}_o$ can be derived as

$$[\mathbf{C_{h_o}}]_{i,j} = \begin{cases}4\sigma_a^2, & i=j\\ 0, & i\neq j\end{cases}.$$

A.3. The MMSE of $\mathbf{h}_o$ and the covariance matrix $\mathbf{C}_{\widehat{\mathbf{h}}_o}(k)$

The probability density distribution of $\widehat{\mathbf{h}}_o$ is Gaussian. We utilize this character and derive the following equation.

$$\mathbf{C}_{\widehat{\mathbf{h}}_o}(k) = (\mathbf{C}_{\mathbf{h}_o}^{-1} + (\mathbf{I}_N\otimes\mathbf{x}^T-\mathbf{A})^T\mathbf{C_e}^{-1}(\mathbf{I}_N\otimes\mathbf{x}^T-\mathbf{A}))^{-1} \tag{22}$$

$$\begin{aligned}&\widehat{\mathbf{h}}_o(k)\\&=\mathbf{C}_{\widehat{\mathbf{h}}_o}(k)((\mathbf{I}_N\otimes\mathbf{x}^T-\mathbf{A})\mathbf{C_e}^{-1}(\mathbf{b}-\mathbf{Sz}-\mathbf{E}\{\mathbf{e}\})+\mathbf{C}_{\mathbf{h_o}}^{-1}\mathbf{h}),\end{aligned} \tag{23}$$

where $\mathbf{x}$ and $\mathbf{z}$ are obtained from previous iteration, and $\mathbf{h} = \begin{bmatrix}-2\mathbf{a}_1^T & \cdots & -2\mathbf{a}_N^T\end{bmatrix}^T$.

A.4. The covariance matrix $\mathbf{C}_\varepsilon$ and $\mathbf{C_F}$

The value of $\mathbf{C}_\varepsilon$ and $\mathbf{C_F}$ could be computed as

$$[\mathbf{C}_\varepsilon]_{i,j} = \begin{cases}4d_i^2\sigma_w^2+2\sigma_w^4+4\sigma_a^4+4\sigma_a^2\|\mathbf{a}_i\|^2, & i=j\\ 0, & i\neq j\end{cases} \tag{24}$$

$$\mathbf{C_F} = \begin{bmatrix}4N\sigma_a^2\mathbf{I}_2 & \mathbf{u}\\ \mathbf{u}^T & \sum_{i=1}^N\sum_{j=1}^N[\mathbf{C}_\varepsilon]_{i,j}\end{bmatrix}, \text{with } \mathbf{u} = \begin{bmatrix}4\sigma_a^2\sum_{i=1}^N[\mathbf{a}_i]_1\\ 4\sigma_a^2\sum_{i=1}^N[\mathbf{a}_i]_2\end{bmatrix} \tag{25}$$

B. REFERENCES

[1] F. L. Lewis, “Wireless sensor networks,” *Smart environments: technologies, protocols, and applications*, pp. 11–46, 2004.

[2] H. P. Tan, R. Diamant, and W. K. Seah, “A survey of techniques and challenges in underwater localization,” *Ocean Engineering*, vol. 38, no. 14, pp. 1663–1676, 2011.

[3] G. Deng, J. Li, W. Li, and H. Wang, “SLAM: Depth image information for mapping and inertial navigation system for localization,” in *Proc. ACIRS*, Tokyo, Japan, July 2016, pp. 187–191.

[4] A. Benlarbi-Delai, J. C. Cousin, R. Ringot, A. Mamouni, and Y. Leroy, “Microwave short baseline interferometers for localization systems,” *IEEE Transactions on Instrumentation and Measurement*, vol. 50, no. 1, pp. 32–39, 2001.

[5] R. M. Vaghefi, and R. M. Buehrer, “Joint TOA-based sensor synchronization and localization using semidefinite programming,” in *Proc. ICC*, Sydney, NSW, Australia, Jun. 2014, pp. 520-525.

[6] R. M. Vaghefi, and R. M. Buehrer, “Cooperative joint synchronization and localization in wireless sensor networks,” *IEEE Transactions on Signal Processing*, vol. 63, no. 14, pp. 3615–3627, 2015.

[7] B. Etzlinger, F. Meyer, F. Hlawatsch, A. Springer, and H. Wymeersch, “Cooperative simultaneous localization and synchronization in mobile agent networks,” *IEEE Transactions on Signal Processing*, vol. 65, no. 14, pp. 3587–3602, 2017.

[8] F. Zhang, G. Wang, and W. Wang, “Novel two-step method for joint synchronization and localization in asynchronous networks,” *IEEE Wireless Communications Letters*, vol. PP, no. 99, pp. 1–1, 2017.

[9] K. W. K. Lui, W. K. Ma, H. C. So, and F. K. W. Chan, “Semi-definite programming algorithms for sensor network node localization with uncertainties in anchor positions and/or propagation speed,” *IEEE Transactions on Signal Processing*, vol. 57, no. 2, pp. 752–763, 2009.

[10] M. Leng, and Y. C. Wu, “Localization of wireless sensor nodes with erroneous anchors via EM algorithm,” in *Proc. GLOBECOM 2010*, Miami, FL, USA, vol. 62, Dec. 2010, pp. 1–5.

[11] Y. Zou, and Q. Wan, “Emitter source localization using time-of-arrival measurements from single moving receiver,” in *Proc. ICASSP*, New Orleans, LA, USA, Mar. 2017, pp. 3444–3448.

[12] Y. Xia, Y. Wang, X. Ma, C. Chen, and X. Guan, “Joint time synchronization and localization for underwater acoustic sensor networks,” in *Proc. WUWNET*, Arlington, VA, USA, Oct. 2015, pp. 1–5.

[13] S. Huffel, and J. Vandewalle, “Analysis and properties of the generalized total least squares problem $\mathbf{AX} \approx \mathbf{B}$ when some or all columns in $\mathbf{A}$ are subject to error,” *SIAM Journal on Matrix Analysis and Applications*, vol. 10, no. 3, pp. 294–315, 1989.